Broadband Impedance Matching Using GRABIM

Here is Part 1 of a description of the Grid Approach to Broadband Impedance Matching (GRABIM) technique

By Thomas R. Cuthbert, Jr.
Consultant

The grid approach to broadband impedance matching (GRABIM) solves the gain-bandwidth design problem. It designs lossless two-port equalizers that match tabulated complex load to complex source impedances for maximum or shaped power transfer over a band of discrete frequencies. Any mix of 12 lumped and distributed element types in a ladder network is allowed.

All reflection functions versus element parameters are unimodal, monotonic, or similar shapes that compose the non-smooth, worst-case reflection envelope over frequency. An efficient grid search using large, medium, and small hypercubes that are repositioned in the solution space reliably locates the likely global minimax solution while avoiding local anomalies in the envelope surface. A final minimax-constrained gradient optimization precisely refines the solution and prunes the topology to produce a reduced-degree full-rank equalizer solution.

Complicated network theory and polynomial mathematics are avoided by using a sure-fire optimization strategy to find solutions that are at least as good as those found by other methods. Program CONETOPM.EXE and a user's guide is available at a small cost.

A fast, simple, and certain means to solve complex broadband matching problems is described and illustrated. Solutions are easily obtained without the need for complicated mathematics. This article emphasizes concepts, the nature of the algorithms, and the kinds of solutions. The details and inexpensive software are available for those wanting to know more.

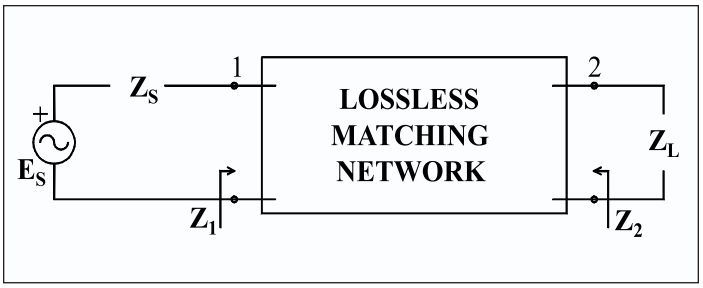

▲ **Figure 1. Broadband matching network terminations and impedances.**

The broadband matching problem

Broadband matching requires design of a matching network (equalizer) placed between a complex source impedance, Z_S, and a complex load impedance, Z_L, as shown in Figure 1. The objective is to transfer as much power as possible over a pass band. Broadband matching networks differ from filters, which have only resistances terminating one or both ports. A broadband matching or gain-bandwidth problem is characterized by having at least one port terminated by a complex impedance function. That is a single-match problem when the other port is terminated by a resistance. A double-match problem has complex impedance functions terminating both ports. GRABIM solves both kinds of problems with the same ease.

The power transfer in Figure 1 is described by equation (1):

$$T \equiv \frac{P_L}{P_{aS}} = 1 - |\rho_1|^2 = 1 - |\rho_2|^2 \qquad (1)$$

where the generalized reflection coefficients are

GHz	Z_S (ohms)	Z_L (ohms)
8.0	108.51–j211.27	9.76–j44.46
9.0	93.53–j197.21	9.63–j38.79
10.0	87.02–j184.93	9.68–j34.84
11.0	71.09–j174.36	9.65–j31.55
12.0	63.50–j164.59	9.68–j28.86
13.0	56.50–j56.23	9.68–j26.52

▲ **Table 1. Yarman impedance data for an interstage network.**

defined as:

$$\rho_1 \equiv \frac{Z_1 - Z_S^*}{Z_1 + Z_S}, \quad \rho_2 \equiv \frac{Z_2 - Z_L^*}{Z_2 + Z_L} \tag{2}$$

P_{aS} is the maximum possible power available from the source ($P_{aS} = |E_S|^2/4R_S$), and P_L is the power delivered to the load. The reflection magnitudes in (1) are called *reflectances* throughout this article. A lossless network maintains constant reflectance at any network interface, especially those adjacent to all its (lossless) internal components.

The terminating impedance functions are usually not known mathematically or by circuit model. Typical terminating impedance data are tabulated versus frequency as illustrated in Table 1. These data are usually obtained by an S-parameter test set. Although Table 1 shows only a single impedance per frequency for each port's termination, there may be a cluster of discrete data defining an *impedance neighborhood* at each frequency. Impedance neighborhoods occur in beam-steered antenna arrays and mobile antennas, and they arise in transistor impedance uncertainty because of either lot variation or operation into saturation.

Conventional methods — Real frequency technique

The real-frequency technique (RFT) originated by Carlin is briefly described, especially its dependence on advanced mathematical considerations and a sequence of less-than-certain optimizations [1], [2]. The RFT was the first advanced technique to consider the practical situation where one or both matching network terminations are characterized only by a tabulation of terminating impedances at a discrete set of frequencies as in Table 1. A piecewise-linear representation of the matching network's Thevenin resistance frequency function $R_2(\omega)$ (see $Z_2 = R_2 + jX_2$ at the load port in Figure 1) over all real frequencies is represented by a sum of weighted basis functions. Because imaginary component X_2 can be determined using the Hilbert transform, Thevenin impedance Z_2 and load impedance Z_L enable calculation of the power transfer at each of the sampled

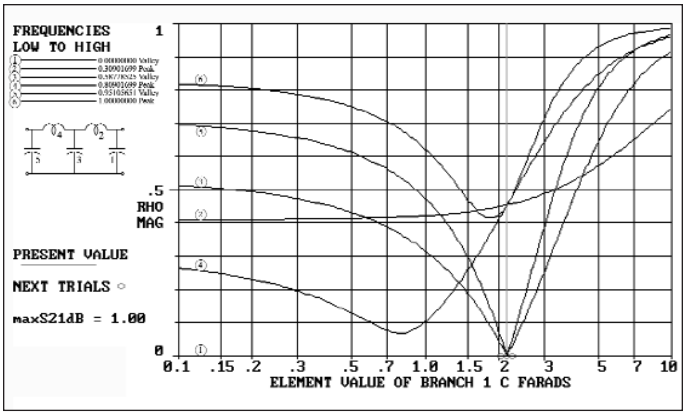

▲ **Figure 2. Reflectance versus Branch 1 C for a fifth degree lowpass filter.**

frequencies according to the preceding equations.

Thevenin resistance function $R_2(\omega)$ has adjustable parameters to optimize the reflectance variation versus frequency. A rational, even resistance function of assumed degree is then fit to the Thevenin piecewise-linear resistance function by a second optimization. Finally, an LC ladder network can be synthesized from the latter function for a resistive source impedance, i.e. the single-match case. Solution of a set of linear equations is required for that synthesis. The double-match case requires a third optimization that includes repeated solution of linear equations. A recent book provides mathematical background and details of the RFT [3].

Reflectance cross sections

Doubly-terminated LC filters are LC two-port networks that have resistive terminations at both ports. It is helpful to observe how the reflectance of such a network behaves as a function of its individual component parameters. For example, a fifth-degree normalized lowpass Chebyshev filter having 1 dB passband ripple can be designed and analyzed to display reflectance $|\rho|$ while varying each of the elements in turn. The cross section graph and annotation in Figure 2 show the result for branch 1, capacitor C_1 that is in parallel with a 1-ohm load resistor (not shown). The abscissa is the value of C_1 over two decades centered on unity, and the ordinate is the reflectance, $|\rho|$, with respect to (wrt) 1 ohm. The nominal (design) value is $C_1 = 2.1349$, and the six curves correspond to the numbered frequencies listed. The six frequencies listed in Figure 1.3.1 are those where the 1-dB passband peaks and the 0-dB valleys occur in the pass band. Other than DC, the remaining two valley frequencies shown have clearly-defined reflection zeros at $C_1 = 2.1349$. Also at $C_1 = 2.1349$, the three curves for the peak frequencies all intersect at $|\rho| = 0.4535$, corresponding to 1.0 dB ripple. Figure 2 is typical of reflectance graphs versus the other network components.

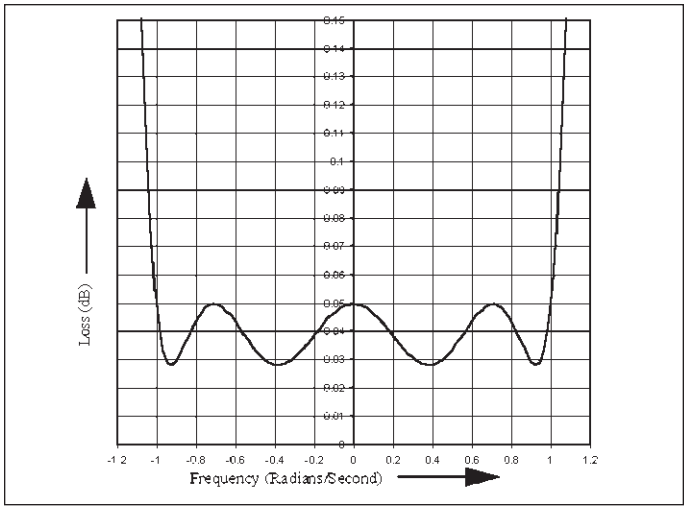

▲ **Figure 3. Normalized lowpass Chebyshev response with flat loss.**

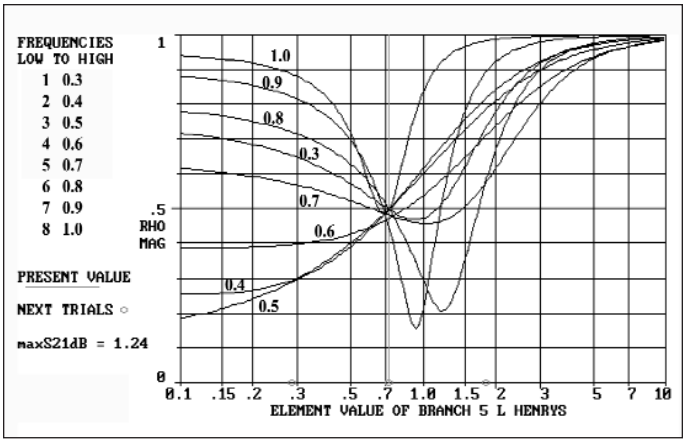

▲ **Figure 4. Typical reflectance functions versus a series branch inductance.**

Iterated analysis for filters

Although conventional synthesis of LC ladder filters in the Laplace *s* plane is badly conditioned numerically, analysis of such ladder networks at discrete frequency samples can be accomplished simply and very accurately. It is also very little extra work to obtain the exact derivatives of the response at those frequencies wrt all the values of ladder elements. Orchard's *iterated analysis* [4] is the automated adjustment of network element values (variables) to obtain reflectance zeros at the proper frequencies. The number of constraints can be made equal to the number of degrees of freedom (variable elements), so there is an exact (nonlinear) solution, i.e. no least-squared error or higher-order compromise is required. Iterated analysis produces element values that are as accurate as those few cases where explicit equations for element values are available.

The frequencies for Chebyshev passband reflection valleys and peaks are easily and accurately obtained by program RIPFREQS.EXE, which is based on formulas by Daniels [5]. Those frequencies are employed in the reflectance cross section graph in Figure 2; thus, two reflectance curves can be made to obtain zero reflectance by automatically adjusting all element values. It is assumed that compatible starting values for each variable are available.

GRABIM strategy

Some filters and all theoretical broadband match responses have *flat loss* in the passband (0.029 dB as shown in Figure 3). Therefore, there are peaks and valleys, but the valleys do not coincide with reflectance zeros, as employed in iterated analysis. In theoretical broadband cases, reflectance valley-frequency curves similar to those in Figure 2 all intersect at some finite reflectance value, and the peak-frequency curves all intersect at some larger reflectance [6]. However, real-world broadband network terminations are not simple, and Chebyshev response shapes are neither optimal nor obtainable, so peak and valley frequencies are not knowable.

In practice, a reasonably uniform set of passband frequencies suffices, and the network elements are automatically adjusted to minimize the maximum reflectance over those frequencies (a *minimax* solution). Typical reflectance cross sections are shown in Figures 4 and 5. These cross sections for LC networks always look the same, even when the elements have not been adjusted — the reflectance value in the "notch" is just greater. The optimization must deal with a non-smooth function, the *envelope*, composed of the upper piecewise arcs displayed in Figures 4 and 5.

GRABIM unfailingly locates and minimizes the notch by an efficient grid search over the elements in order to

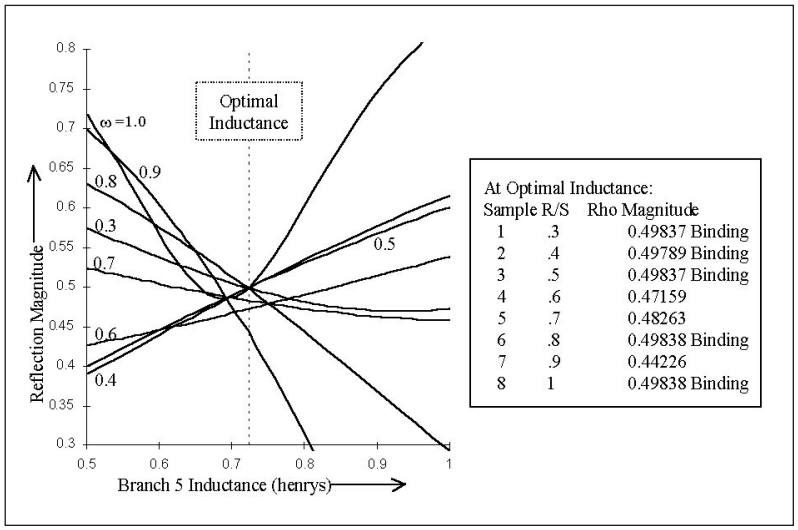

▲ **Figure 5. Closeup of binding and nonbinding reflectance functions.**

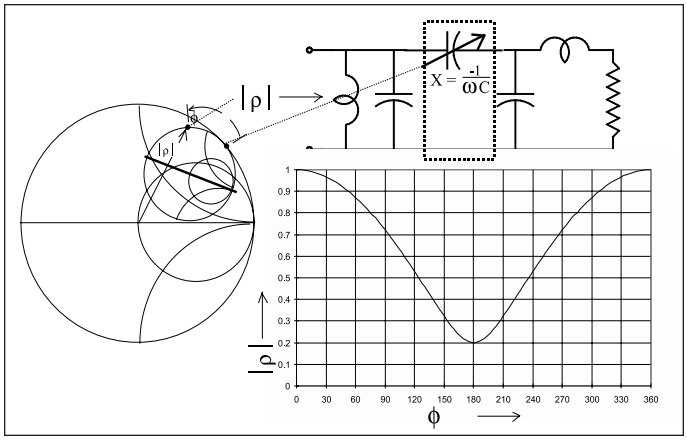

▲ **Figure 6. Origin of all ρ_i reflectance curves versus branch X values.**

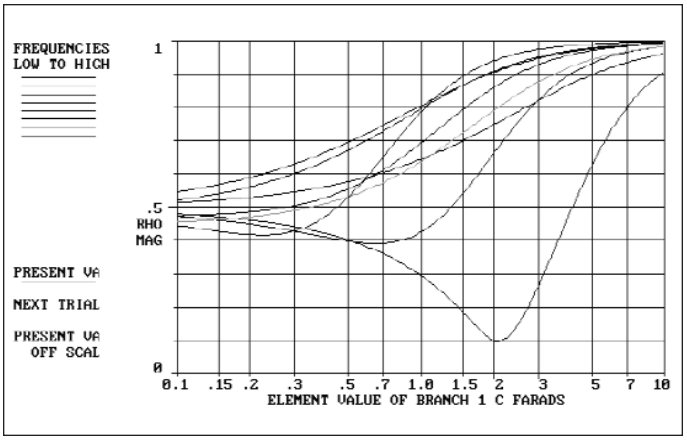

▲ **Figure 7. A monotonic envelope function for a branch leaving the solution.**

prepare for the gradient method of multipliers. The latter accurately solves constrained nonlinear optimization problems when started near a solution. Fortunately, minimization of the non-smooth envelope function in Figure 5 can be converted into minimization of a simple smooth function subject to smooth constraints.

Equalizer networks

All reflectance functions versus element parameters are unimodal, monotonic, or similar shapes that compose the worst-case reflection envelope over frequency. A unimodal function (smooth or not) has only one minimum. A monotonic function declines steadily and has no definite minimum. This section shows why the reflectance cross sections for all element parameters have benign shapes typified in Figure 4.

Lumped element reflectance functions

Curves in Figures 2, 4, and 5 have the same benign appearance for a good reason: Input reflection coefficient ρ_1, equation (2), of a linear network is a bilinear function of network branch impedances [6]. Bilinear functions map lines in impedance planes into circles in reflection planes, e.g. into a Smith chart.

Figure 6 illustrates how a varying series-branch capacitance affects the input reflection coefficient plotted on a Smith chart for some frequency. If the capacitance is zero, the input LC pair causes a unit reflection which is a point somewhere on the edge of the chart. All other positive and negative values of C generate the circular reflection locus, the rim of a smaller Smith chart, which may or may not encircle the center of the larger Smith chart.

Figure 6 also shows a graph of the magnitude of the polar vector terminating on the circular locus as a function of ϕ, the angle around the rim of the smaller Smith chart. The unimodal curve of $|\rho|$ versus ϕ is the origin of all the LC reflectance curves above. There is a nonlinear, monotonic relationship between element value C and ϕ, which distorts the reflectance cross sections horizontally.

A reflectance cross section commonly observed is

Type	Code	Name	Variables	Constant
1	CS	Series capacitor	C	
2	LP	Parallel inductor	L	
3	LS	Series inductor	L	
4	CP	Parallel capacitor	C	
5	LCS	Parallel LC in series	L	ω_∞
6	LCP	Series LC in parallel	C	ω_∞
7	XFMR	Ideal transformer	t^2	
8	CASTL	Cascade transmission line	Z_0,θ_0	ω_0
9	SCS	Short-circuit stub in series	Z_0,θ_0	ω_0
10	SCP	Short-circuit stub in parallel	Z_0,θ_0	ω_0
11	OCS	Open-circuit stub in series	Z_0,θ_0	ω_0
12	OCP	Open-circuit stub in parallel	Z_0,θ_0	ω_0

▲ **Table 2. Twelve lossless ladder network elements and parameters.**

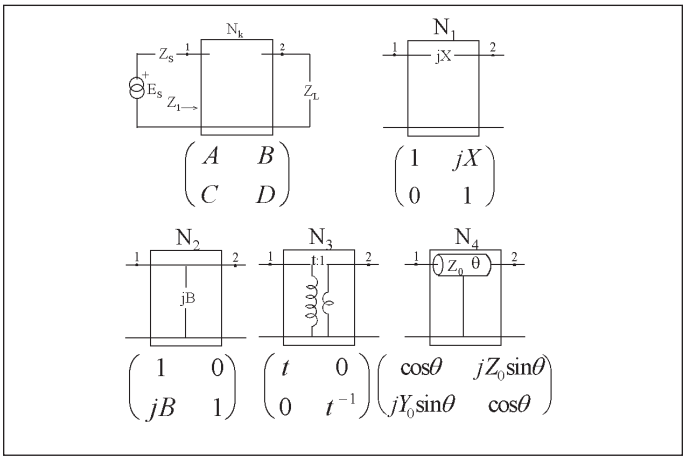

▲ **Figure 8. All lossless subnetworks for interface reflection analysis.**

shown in Figure 7. In that situation, the value of a parallel-branch capacitance (decreasing from $C \rightarrow \infty$ on the Smith chart edge) fails to drive ϕ beyond 180 degrees on those piecewise arcs composing the worst-case envelope. A precise search algorithm that minimizes the envelope also forces that C to zero, automatically pruning that branch from the network.

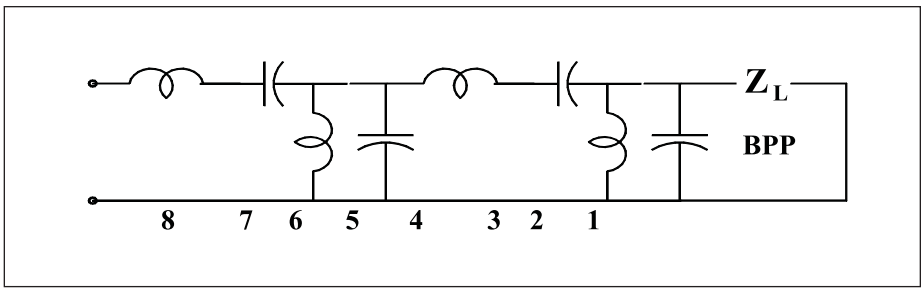

▲ **Figure 9. A bandpass topology with the first element in parallel with the load.**

Element reflectance behavior

Earlier, it was shown that the reflectance is constant at any interface in a lossless network. Figure 8 shows that any subnetwork, N_k, embedded in a matching network will be terminated with its own Thevenin-equivalent source and load at its interfaces. Subnetworks N_1 through N_4 account for all types of elements allowed: L, C, LC transmission zeros (stopband traps), ideal transformer, and cascade and stub transmission lines. Figure 6 explains the reflectance function caused by subnetwork N_1 in Figure 8; subnetwork N_2 is just the dual case. The ideal transformer, N_3, also produces a unimodal reflectance versus its turns ratio. Cascade transmission line (CASTL) element N_4 is only slightly different. Its reflectance versus electrical length, θ, also generates a circle in the Smith chart, similar to that in Figure 6, but not touching the chart edge. The CASTL reflectance versus its characteristic impedance, Z_0, is either unimodal or bimodal (two minima). The analysis of these effects and the fact that they do not invalidate either the grid search or subsequent gradient optimization have been demonstrated [6].

Lossless network topologies

Table 2 lists all 12 ladder network elements, the respective parameters that are varied during optimization, and those that remain constant. Each element fits one of the four basic subnetworks described in Figure 8. Broadband matching theory shows the need for only limited

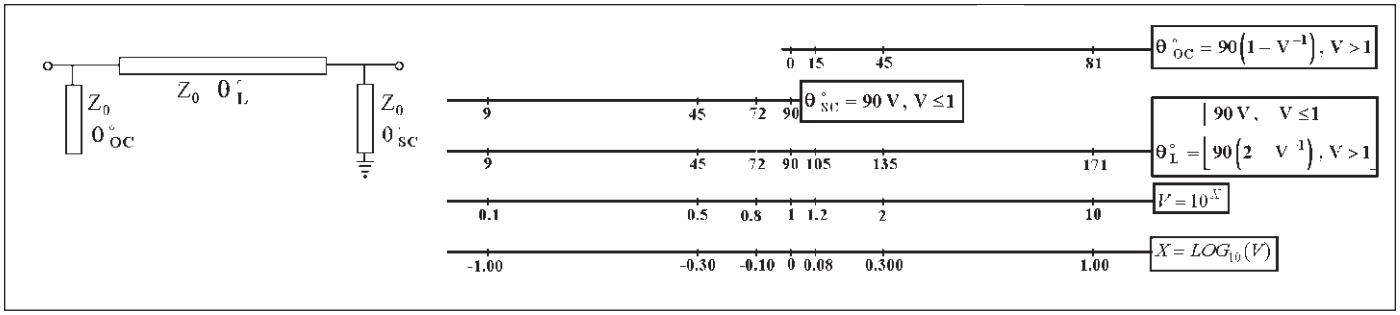

▲ **Figure 10. Three kinds of transmission-line elements and mappings.**

equalizer degree, so program CONETOPM.EXE accommodates up to ten variables and stores 12 candidate LC network topologies for speedy trials. For example, Figure 9 shows eight branches (elements) in a standard bandpass topology that begins with a parallel branch across load Z_L. (Element numbering is from the load toward the source.) Any number of elements from 2 to 10 can be specified, e.g., BPP8 is the network illustrated. Although the user can use topology codes (Table 2) to enter different candidate lowpass or bandpass matching networks, having a standard set of candidate networks available is expeditious. Figure 10 shows three kinds of distributed elements. Stubs are usually separated by a CASTL which is less than 180 degrees. The open-circuit stub on the left and the short-circuit stub on the right are usually less than 90 degrees. Ten variables can accommodate five distributed elements, each having two parameters.

Scaling and mapping variables

To obtain well-scaled response surfaces, it is necessary to scale the effects of variables, i.e. values of L, C, squared turns ratio t^2, Z_0 and θ_0. Because normalization to 1 rad/s and 1 ohm is required, units are henrys, farads, numeric, ohms, and degrees (θ_0) at 1 rad/s, respectively. Practical ranges of variables are shown in Figure 10 for V, as suggested by theoretical broadband Chebyshev network element values [7, pp. 126-129]. The branch cross sections displayed, e.g. Figure 4, utilize L, C, t^2, and Z_0 values in the log-

arithmic V space, which is simply related to the linear X space as shown in Figure 10.

Unbounded gradient optimization in the X space automatically ensures positive element values in the V space, because that amounts to quantifying variables in dB. Also, gradient optimization in the X space is optimally scaled, producing derivatives normalized like Bode sensitivities. A value in V also may define a corresponding value of θ_L, θ_{SC}, or θ_{OC} (at ω=1 rad/s), according to the equations beside the top three lines in Figure 10. Stubs are related to a split range of V to facilitate a grid search being able to select optimally either a short- or an open-circuit stub. The values of electrical length shown in Figure 10 are those at the defined reference frequency of $\omega_0 \equiv 1$ rad/s. Therefore, the variable is θ_0, with the understanding that at any other frequency the actual electrical length, θ, is linearly related to θ_0.

Grid search

The grid search on and within large, medium, and small hypercubes that are repositioned in the solution space approximately locates the likely global minimum while avoiding local anomalies in the envelope surface. See Figure 4. The methodical grid searches each coordinate in the vicinity of the normalized domain where classical broadband theory show all possible answers exist, $0.09 \le V \le 12.0$. It is a 1950's method enhanced by 1990's research [8].

Non-smooth objective function

It is computationally convenient to deal with the inverse of the relative load power defined in (1); therefore, define:

$$P \equiv \frac{P_{aS}}{P_L} = \frac{1}{1-|\rho|^2} \ge 1 \qquad (3)$$

Suppose there is a candidate network and a vector of values, x, each component defined in the domain at the bottom of Figure 10. Consequently, all network element values, vector v, are known, so analysis at a set of frequencies, ω_i, i in the set I, yields a corresponding set of P_i. There may be a finite goal or target for P_i at the ith frequency, say g_i, which is obtained from desired loss L_i by:

$$g_i = 10^{L_i/10},\ L_i \text{ in dB at } \omega_i \qquad (4)$$

Over all the sample passband frequencies and trial variables there will be a maximum value of P, say P_{max}. The nonsmooth minimax objective for the grid search is:

$$\underset{Over\ x}{Minimize}\ P_{\max} \text{ subject to: } \max_{i \in I}\left[(P_i - g_i) - P_{\max}\right] \le 0 \qquad (5)$$

Equation (5) says that the error at

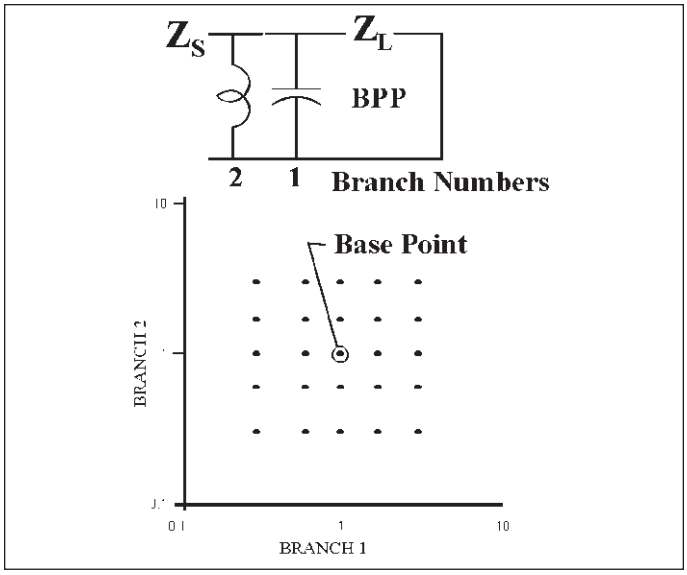

▲ **Figure 11. A 5×5 lattice (grid) for a two-branch matching network.**

each frequency should be less than some value P_{max}, and that P_{max} should be made as small as possible by varying all values in vector x.

Lattices

A grid search tests combinations of element values in a candidate network to obtain an approximate solution of the minimax matching objective stated in (5). It is basically a search in coordinate directions, Figure 11, using a fixed set of discrete values for each element. The best combination in the grid (lattice) is found, then the grid's base point is recentered there in each coordinate direction. Grid evaluation and repositioning are continued until no further reduction of P_{max} can be found in that grid. The spacing between grid points (granularity) is then reduced, and the evaluation and repositioning process is repeated. Usually, only two or three repositions are required for each grid, and only three reductions in granularity (spacing) are required to arrive in the neighborhood of the likely global minimum. The benign nature of the envelope reflectance curves, recent research results in pattern-search optimization, fast PCs, and efficient implementation make grid searches feasible [6].

The grid defined for the two-element network in Figure 11 has five discrete values logarithmically centered on unity (the best guess available) for each branch's L and C value. Linear patterns of points on X produce these logarithmic patterns on V in Figure 10. The algorithm is as follows: Test each of the 25 combinations of the element value set {1, 0.6, 1.7, 0.3, 3} for each branch at each passband frequency sample. Beginning with L = 1 and C = 1, compute P_{max} for each frequency, and store the greatest (worst) value of P_{max} at any frequency with the corresponding L and C values as the "best case." Then try L = 1 and C = 0.6; if the greatest P_{max} versus frequency is less than the stored value, then store that and the branch values as the best case. A frequency scan is abandoned whenever P_{max} at any frequency exceeds the stored best case, because that LC combination has thus failed. Next try L = 1 and C = 1.7, etc., until all five branch 1 values have been tried. Then set L = 0.6 in branch 2, and go through the branch 1 set again. One of the 25 points in Figure 3.2.1 is the best case (minimax) for this iteration. For each frequency there could be yet another loop to process multiple impedances that define an impedance neighborhood.

A grid search in two dimensions locates a minimum in a surface such as that illustrated in Figure 12. A grid (lattice) is analogous to an archeologist's coordinate frame positioned near a hole. Depending on the depth read at each coordinate intersection, the lattice is repositioned until no lattice point yields a greater depth. The lattice is alternately downsized and then repositioned a few more cycles until the bottom of the hole is suitable located.

Unlike some popular direct search methods, this grid search is not opportunistic: it makes no speculative iterate based on results from previous iterates, so it avoids being trapped by anomalies (local minima and valleys). A full search over a coarser grid is usually more efficient in locating an optimal point than a random search. Another advantage of the GRABIM search algorithm is that, unlike the popular Nelder-Mead simplex algorithm, it is backed by convergence theorems that are borne out in practice by numerical tests [8].

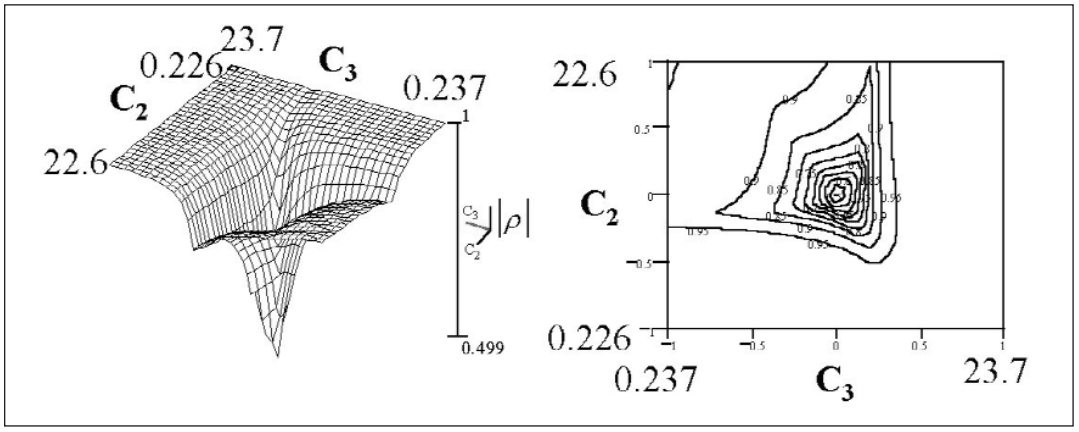

▲ **Figure 12. A typical response surface in two-space for a grid search.**

The task of validating the global solution to a general optimization problem is very difficult. In spite of the unimodal/monotonic behavior in coordinate directions, the minimax objective function can be assumed to be neither convex nor concave, having multiple local minima. However, the grid search is essentially a coordinate search of known functions, so it always locates the global solution along parameter coordinates. Furthermore, extensive testing along hypercube principal diagonals has never found better solutions, thus the claim of a likely global solution [6].

Efficient Search

Figure 11 illustrates a k^n *factorial search*, where k = 5 and $n = 2$. Because of the exponential increase in computing time with n variables, program CONETOPM.EXE employs k = 5 for $n \le 4$, k = 3 for $5 \le n \le 6$, and K = 2 for $7 \le n \le 10$. Grid searches on a 200 MHz PC require less than 15 seconds while making 10 to 50 thousand trials. There are several important techniques for increasing efficiency in addition to abandoning a frequency scan whenever P_{max} at any frequency exceeds the stored best case. The power transfer function in (3) is computed by:

$$P = |H|_2 \tag{6}$$

where:

$$H \equiv \frac{A\,Z_L + jB + jC\,Z_S + D\,Z_S}{2\sqrt{R_L\,R_S}}$$

Terms A, jB, jC, and D in (6) are the chain parameters of the complete lossless candidate matching network, and are obtained using the ABCD parameters for each component, Figure 8.

Ladder network analysis is performed by Orchard's chain matrix technique [4], which need not be repeated at each frequency when multiple load and/or source impedance data defines a neighborhood. Current PCs perform basic operations (add, subtract, multiple and divide) in about 1 microsecond. Orchard's method requires only four or eight operations to incorporate each network element while evaluating the overall ABCD network matrix. The exact partial derivatives of the overall ABCD matrix with respect to all element values (required below) are obtained in only two network analyses at each frequency. Precomputation of ladder branch reactances before each grid search iteration vastly increases grid search efficiency, because frequency samples are fixed and every possible parameter value is known for each lattice. ■

To be continued next month

This in-depth article requires more space than is available in this issue. The article will continued in the next issue with the conclusion of solution search techniques, examples and concluding remarks. The entire list of references is included here, and will be repeated following Part 2.

Copyright notice

References

1. A. N. Gerkis, "Broadband Impedance Matching Ysing the "Real Frequency" Network Synthesis Technique," *Applied Microwave & Wireless*, V10N6, July 1998, pp. 26-36.

2. H. J. Carlin, "A new approach to gain-bandwidth problems," *IEEE Trans. Circuits and Systems*, V24N4, April 1997, pp. 170-175.

3. H. J. Carlin and P. P. Civalleri, *Wideband Circuit Design*, CRC Press, 1998.

4. H. J. Orchard, "Filter design by iterated analysis," *IEEE Trans. Circuits and Sys.*, V32, N11, Nov. 1985, pp. 1089-1096.

5. R. W. Daniels, R. W. (1974). Approximation Methods for Electronic Filter Design. NY: McGraw-Hill.

6. T. R. Cuthbert, *Broadband Direct-Coupled and Matching RF Networks*, TRCPEP Publishing, 1999.

7. G. L. Matthaei, L. Young, and E. M. T. Jones, *Microwave Filters, Impedance Matching Networks, and Coupling Structures,* McGraw-Hill 1964. Also, Artech House, 1980.

8. V. Torczon, "On the convergence of pattern search algorithms," *SIAM J. Optimization*, V7N1. Feb 1997, pp. 1-25.

9. M. J. D. Powell, "A method for nonlinear constraints in minimization problems," in *Optimization*, R. Fletcher, Ed., Academic Press, 1969, pp. 283-297.

10. T. R. Cuthbert, "Optimization Using Personal Computers with Applications to Electrical Networks," John Wiley & Sons, 1987.

11. T. R. Cuthbert, *User's Guide for CONETOPM, Version 990120*. TRCPEP Publishing, 1999, 25 pages.

12. P. L. D. Abrie, "The transformation-Q approach to synthesizing lumped-element impedance-matching networks," *Suid-Afrikaanse Tydskrif vir Wetenskap*, V89, March/April 1991, pp. 147-149.

13. L. Urshev, L. and A. Stoeva, "A program for the design of Chebyshev impedance-transforming lowpass filters." *RF Design*, May, 1994, p. 76.

Author information

Tom Cuthbert can be reached at 975 Marymount Drive, Greenwood, AR 72936, tel: 501-996-5713; fax: 501-996-5618; e-mail: TRCPEP@aol.com